Journal of Neuroimaging in Psychiatry & Neurology

https://doi.org/10.17756/jnpn.2021-039

Research Article

Open Access

Medial Temporal Lobe and Cortical Involvement: Neuroanatomical Signatures of Symptom Dimension Dominant Schizophrenia

Rakshathi Basavaraju, Xinyang Feng, Jeanelle France and Frank A. Provenzano*

Department of Neurology, Taub Institute for Research on Alzheimer's Disease and the Aging Brain, Columbia University Medical Centre, New York, USA

***Correspondence to:**
Frank A. Provenzano, PhD
Assistant Professor of Neurological Sciences
Taub Institute for Research on Alzheimer's Disease and the Aging Brain, Department of Neurology, Columbia University Medical Centre
New York, USA
E-mail: frank.provenzano@columbia.edu

Received: July 15, 2021
Accepted: September 03, 2021
Published: September 05, 2021

Citation: Basavaraju R, Feng X, France J, Provenzano F. 2021. Medial Temporal Lobe and Cortical Involvement: Neuroanatomical Signatures of Symptom Dimension Dominant Schizophrenia. *J Neuroimaging Psychiatry Neurol* 6(1): 7-16.

Published by United Scientific Group

Abstract

Aims: Schizophrenia is a psychiatric disorder with diverse clinical presentations that have differential prognoses and treatment responses. We aimed to explore the differences in neuroanatomical patterns between groups of schizophrenia having different symptom dimensions from an openly available neuroimaging source.

Methods: T1-weighted MRIs and symptom ratings (SAPS – Scale for Assessment of Positive Symptoms & SANS – Scale for Assessment of Negative Symptoms) were obtained from the open database SchizConnect (http://schizconnect.org/). Based on standard symptom remission criteria, subjects were grouped into Positive symptoms (*n*=29) and Negative symptoms predominant (*n*=84) groups and healthy controls (*n*=120). Structural-MRI analysis was performed on Freesurfer and the scanner site-harmonized brain volumes were compared across the 3 groups.

Results: Negative-Predominant group compared to healthy controls had smaller bilateral hippocampus, right amygdala, left thalamus, bilateral superior frontal, right parsopercularis, right parstriangularis, bilateral middle temporal, left parahippocampal, left entorhinal, bilateral fusiform, bilateral superior parietal and left inferior parietal cortex. In contrast, the Positive-Predominant group demonstrated volumetric reductions in bilateral hippocampus, bilateral parahippocampal and left entorhinal cortex only, compared to healthy controls.

Conclusions: Exclusive bilateral medial temporal lobar volumetric reduction underlies positive symptoms, but additional extensive cortical and subcortical volume loss underlies negative symptoms. Symptom dimensions rather than standard diagnostic entities have distinct neuroanatomical signatures implying significant heterogeneity within the diagnosis. .

Keywords

Schizophrenia, Positive symptoms, Negative symptoms, Structural MRI, Symptom dimensions, Brain volumes, Grey matter

Introduction

Schizophrenia is a chronic debilitating psychiatric disorder that has a prevalence of approximately 0.5% of the US adult population [1], with an estimated global burden of 13.4 million years of life lived in disability secondary to the disease [2]. Schizophrenia is characterized by significant heterogeneity in its clinical presentation [3] comprising of positive symptoms like delusions and hallucinations; negative symptoms like affective flattening, alogia, apathy,

anhedonia; and, also cognitive and mood symptoms. The heterogeneity is not just restricted to the symptomatic presentation, but also dictates treatment response [4, 5] and prognosis of the disorder [6-8] with negative symptoms and cognitive deficits contributing to substantial disability [9] with poorer response to conventional treatments [10], thus emphasizing the need to understand and address the underlying drivers of heterogeneity better.

The differences in schizophrenia phenotypes are also reflected in many neurobiological substrates underlying pathophysiological basis of schizophrenia. These have been studied using structural neuroimaging [11, 12], functional neuroimaging [13] and genetics [14]. A multitude of differing imaging findings in different studies of schizophrenia [11] has been attributed to the diversity of phenotypes (Wheeler et al.) which emphasizes the importance of understanding the specific associations of symptoms and structural brain findings. There is evidence pointing towards different patterns of structural magnetic resonance imaging (MRI) findings in the brain with different symptomatic subtypes, with most of the studies indicating a differential involvement of the frontal and temporal cortices, subcortical structures like the thalamus and cerebellum, as well as differences in magnitude and extent of cortical and subcortical volumetric aberrations between the symptom subgroups [12, 15-21]. Large meta-analyses associate the positive symptoms of schizophrenia to thinning at bilateral superior temporal gyri [22] whereas, the negative symptoms to thinning at left medial orbitofrontal cortex [23], potentially implying that different sub regions of the brain govern different symptom subsets of schizophrenia. Some of the latest studies employing advanced methods like machine learning to differentiate schizophrenia from healthy population with possible structural MRI-derived patterns, report data-driven subtyping of the imaging data that is associated with different kinds of symptoms as well as an increase in classification accuracy of the algorithm after subtyping [24]. Another study employing machine learning techniques showed that negative symptom severity was significantly associated with the probability of individual scans being classified as schizophrenia or not [25]. Given this background of heterogeneous symptomatology guiding brain structural MRI findings, we examined structural patterns of the cortex and sub-cortex in individuals with symptomatic schizophrenia by subgrouping them using a clinically derived symptom-predominance pattern on a varied public and open neuroimaging database.

Methods

Acquisition of imaging data

We chose the open database SchizConnect (http://schizconnect.org/) as our source of neuroimaging data, which offers access to investigators of MRIs of schizophrenia subjects from multiple projects. We obtained data from 4 projects i.e., The Center for Biomedical Research Excellence (COBRE), functional imaging Biomedical Informatics Research Network (fBIRNPhaseII__0010 (UCI_HID)), MIND Clinical Imaging Consortium (MCICShare) and the Northwestern University Schizophrenia Data and Software Tool (NUSDAST). These projects comprise of multiple modalities of neuroimaging and clinical assessments [26-29]. We restricted our search to only those subjects who had concurrent T1-weighted MRI and clinical assessments at a baseline visit of every individual study. This search yielded us 420 subjects who had concurrent baseline T1-weighted MRI and clinical assessments. The entire process of obtaining the MRIs and arriving at the final sample has been described in figure 1. Specific T1-weighted MRI acquisition parameters of the 4 projects are mentioned in the supplemental figure 1.

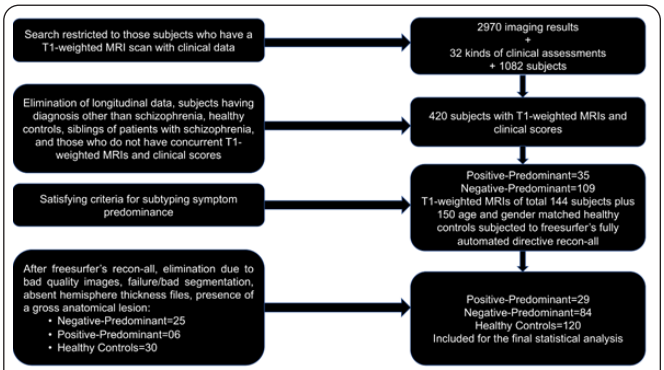

Figure 1: Flow diagram depicting the process of selection of subjects (T1-weighted MRIs, demographic and clinical data) from the open database SchizConnect (http://schizconnect.org/).

Subjects

The projects included subjects with a Diagnostic and Statistical Manual of Mental Disorders, 4th edition (DSM-IV) diagnosis of Schizophrenia. Kindly refer to the supplemental methods 1, "Inclusion and exclusion criteria of subjects" for a description of the criteria of individual projects.

Symptom ratings

The symptom ratings provided by the fBIRNPhaseII__0010, MCICShare and NUSDAST were the Scale for the Assessment of Positive Symptoms (SAPS) and Scale for the Assessment of Negative Symptoms (SANS) [30] whereas, COBRE provided the same in Positive and Negative Symptom Scale (PANSS) [31]. For the sake of uniformity of classification of subjects to symptom-predominant subgroups we derived SAPS Global Summary Score and SANS Global Summary Score from the PANSS ratings of COBRE using the conversion equations as described by van Erp et al., 2014 [32]. The SAPS and SANS global summary scores were derived from summation of the global scores of the individual items of SAPS (items 7, 20, 25 and 34) and SANS (8, 13, 17, 22 and 25) respectively in the other 3 projects. So, each subject had 2 items, one SAPS Global Summary Score and another a SANS Global Summary Score.

Classification of subjects into symptom predominant subgroups

Clinical classification based on standard remission criteria

We classified subjects into 2 groups i.e. one with predominant positive symptoms of schizophrenia (Positive-Predominant/PP) and one with predominant negative

symptoms of schizophrenia (Negative-Predominant/NP) based on the standard remission criteria of scoring 2 or less on each of the global items individually on SAPS (4 global items) and SANS (5 global items) [33]. Hence, we classified subjects having a SAPS global summary score of more than 8 (scoring just 2 on each of the 4 SAPS items) and a SANS global summary score of less than or equal to 10 (scoring just 2 on each of the 5 SANS items) as PP whereas, subjects having a SANS global summary score of more than 10 and a SAPS global summary score of less than or equal to 8 as NP, yielding 2 clearly distinguishable groups. Thus, the PP had a remission of negative symptoms, and the NP had a remission of positive symptoms. Finally, 233 subjects were analyzed (PP = 29, NP = 84, Healthy Controls/HC=120) (figure 2).

Classification based on an unsupervised machine learning algorithm (k-means clustering)

We performed k-means clustering, an unsupervised machine learning algorithm on all the 420 subjects. We categorized the subjects into 3 clusters (number of clusters deemed suitable for the given data as indicated by elbow method based on the minimization of total within cluster sum of squares/WSS) based on their SAPS and SANS global summary scores. The clusters created by the k-means algorithm had subjects belonging to all 4 clinical categories (fully remitted, subjects having both kinds of symptoms, positive symptoms, and negative symptoms). As we wanted to examine only those subjects who exclusively had either positive or negative symptoms, we decided to adopt the clinical classification. We found a high concordance between the clinical classification based on standard remission criteria and the classification as per k-means clustering algorithm, as indicated by statistical comparison of the groups created by the respective methods ($p<0.001$). We also observed a high concordance between the final symptom-predominant groups created by the clinical classification (29PP and 84NP) and the k-means clusters to which the same subjects belong to ($p<0.001$). Thus, an agnostic clustering machine learning algorithm validated the clinical classification, establishing it as a sound method of subject categorization into symptom predominant subtypes (Figure 2).

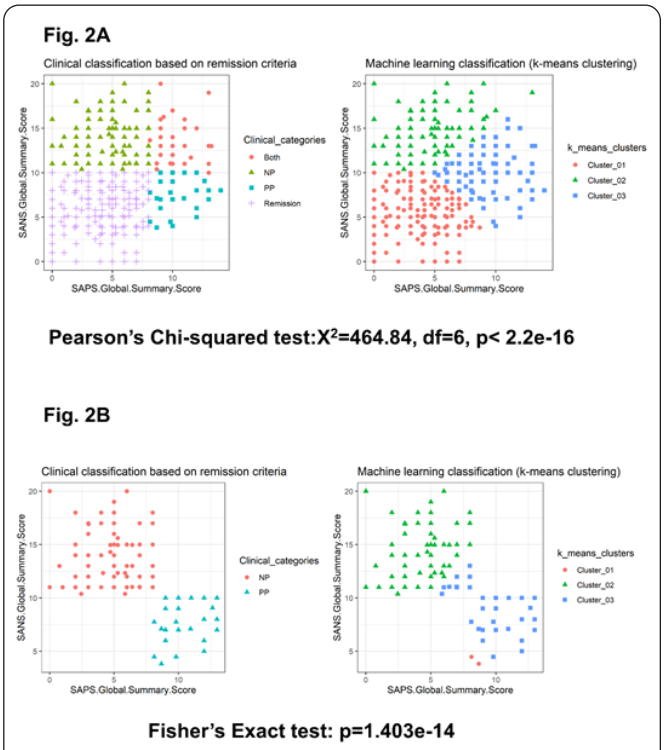

Figure 2: Figure 2A**:** Scatterplots of the SAPS and the SANS global summary scores of the entire sample (N=420) categorized according to clinical classification as per remission criteria and k-means clustering algorithm. The groups obtained by the respective methods are concordant as indicated by statistical similarity as per a significant Chi-square test ($p<2.2e-16$). Figure 2B: Scatterplots of the SAPS and the SANS global summary scores of the patient sample used for final statistical analysis (29 PP, 84 NP) categorized according to clinical classification as per remission criteria and k-means clustering algorithm. The groups obtained by the respective methods are concordant as indicated by statistical similarity as per a significant Fisher's exact test ($p=1.403e-14$).
SAPS= Scale for Assessment of Positive Symptoms, SANS= Scale for Assessment of Negative Symptoms, PP= Positive-Predominant Schizophrenia defined as SAPS global summary score>8 and a SANS global summary score≤10, NP=Negative-Predominant Schizophrenia defined as SANS global summary score>10 and a SAPS global summary score≤8. Both= SAPS global summary score>8 and SANS global summary score>10. Remission= SAPS global summary score≤8 and SANS global summary score≤10. df=degrees of freedom.

Structural imaging analysis

Volumetric analysis

Using Freesurfer 6.0, an open source brain MRI analysis software, we obtained brain volumetric measurements from T1-weighted MRIs of subjects. A quality check on the T1-weighted images comprised of careful visual inspection with elimination of those with poor-quality. Images were determined to be of poor-quality if they were poor on one or more of the following criteria: field of vision, grossly obvious head motion, inhomogeneity artefacts and presence of gross anatomical lesions. Also, images with gross topological defects (observed after freesurfer processing) were also eliminated. The raw images which passed through the process of quality check were subjected to skull stripping and intensity normalization as a part of image pre-processing. The analysis was completed using 3 processes: cortical surface reconstruction, cortical parcellation and subcortical segmentation. **Cortical surface reconstruction:** The topology of cortical surfaces was algorithmically corrected by Freesurfer [34-36]. This reconstruction step transformed the intrinsically irregular cortical surface into a smooth coordinate plane by inflation and flattening techniques. A matrix was constructed which stored these transformation patterns and subsequently coordinated into Talairach space [37] which was utilized for further analysis [38].

Cortical parcellation

Freesurfer's cortical parcellation algorithms [38] automatically generated volumetric measurements of unique cortical gyri and sulci structures utilizing the Desikan-Killiany-Tourville brain atlas as a reference [39, 40].

Subcortical segmentation

This process automatically yielded volumetric measurements of subcortical neuroanatomical structures where neuroanatomical labels were assigned to each voxel in the pre-processed T1-weighted MRI [41]. We obtained volumetric measurements of 60 bilateral brain areas through this analysis pipeline (Table 2), and these brain areas were compared between the groups.

Harmonization of structural MRI measurements across sites

As we are including T1-weighted MRIs from 4 different projects it is crucial to account for the differences in scanners and image acquisition protocols across sites. We used ComBat, a batch-effect correction tool originally used in genomics [42] which corrects for variance introduced by non-biological confounders like differential scanners and parameter configurations that are known to have apriori unpredictable effects. By using an empirical bayes framework this tool performs better than adjusted residuals harmonization (adding project site as a covariate in the linear regression model) as it also accounts for site-specific scaling factors [43]. ComBat has been utilized to harmonize multi-site diffusion tensor imaging data [43] and also cortical thickness measurements in 2 large multi-site studies across 11 scanners [44]. It has the property of preserving the variance in the data due to true biological factors and removing just the batch effects provided that the biological variables are also passed on to the algorithm. We used the ComBat software freely available for R (R Studio version 3.6.0) (https://github.com/Jfortin1/ComBatHarmonization/tree/master/R#id-section1) with project site (COBRE, fBIRNPhaseII__0010, MCICShare and NUSDAST) as the batch variate, age, gender, estimated intracranial volume and group as the biological variables and obtained modified site-adjusted volumetric measurements on which further statistical analyses were performed.

Statistical analysis

Age, gender, and the projects were compared across the 3 groups with Analysis of variance (ANOVA) and chi-square tests accordingly. The ComBat-corrected volumes of cortical and subcortical structures were compared across the 3 groups using Analysis of Covariance (ANCOVA) with age, gender and estimated intracranial volume (ETIV) as covariates in the model. If the group difference was significant in the ANCOVA, post-hoc analyses to know the inter-group differences were performed using Bonferroni test. As the sample sizes were unequal we used the Welch's ANOVA for the main effect and dunnettT3 test as the post-hoc test for those volumes which had unequal variance across the 3 groups, as indicated by Levene's test [45]. The p value of the group difference in the ANOVA (ANCOVA/Welch's ANOVA) was corrected for multiplicity of brain areas using the Benjamini-Hochberg/False Discovery Rate (FDR) method [45]. The level of alpha was fixed as 0.05. All statistical analyses were performed using the software, R Studio version 3.6.0.

Ethical approval and consent

The study was determined to be exempt of review by the Institutional Review Board (Reference number: IRB-AAAS6975).

Results

Sociodemographic and clinical variables

There were no significant differences between the 3 groups with respect to age, gender, and the proportional contribution of subjects from the individual projects (Table 1).

Comparison of subcortical and cortical volumes between the 3 groups

ANCOVA/Welch's ANOVA showed that multiple areas were significantly different across the groups. Volumes of the following structures were lesser in NP compared to HC: bilateral hippocampus, right amygdala, left thalamus, bilateral superior frontal, right parsopercularis, right parstriangularis, bilateral middle temporal, left parahippocampal, left entorhinal, bilateral fusiform, bilateral superior parietal and left inferior parietal cortex (Figure 3). In contrast to the widespread loss of cortical and subcortical tissue in

Table 1: Sociodemographic and clinical variables.

	PP	NP	HC	F/X^2	*p*
†**Age(years)**	35.9(11.99)	33.22(12.54)	35.04(13.22)	0.699	0.4977
‡**Gender(Males)**	72.41	78.83	66.94	3.494	0.1743
‡**SchizConnect Project**	NUSDAST = 34.5	NUSDAST = 48	NUSDAST = 40.5	5.898	0.4346
	fBIRN = 7	fBIRN = 1	fBIRN = 6.6		
	COBRE = 27.5	COBRE = 18	COBRE = 19		
	MCICSHARE = 31	MCICSHARE = 33	MCICSHARE = 33.9		

PP = Positive-Predominant, NP = Negative-Predominant, HC = Healthy Control
F = F statistic of Analysis of Variance (ANOVA), X^2 = Chi-square test
†Mean (Standard Deviation)
‡Percentage

NP, the PP group demonstrated lesser volumes only in the bilateral hippocampus, bilateral parahippocampal and left entorhinal cortex compared to healthy controls (Figure 4, 5, Supplementary Figure 2). Apart from left parstriangularis being smaller in NP compared to PP at trend level post-hoc significance (Bonferroni test p = 0.08) there were no other differences between these 2 groups (Table 2).

Table 2: Comparison of subcortical and cortical volumes between the 3 groups (PP, NP, Controls).

Structure	Left			Right		
	F(df)	$*p_{FDR}$	Post-hoc	*F(df)*	$*p_{FDR}$	Post-hoc
Hippocampus	9.99 (2,229)	0.003	PP<HC NP<HC	8.75 (2,78.87)	0.008	PP<HC NP<HC
Amygdala	2.81 (2,86.11)	0.099		5.24 (2,229)	0.023	NP<HC
Thalamus	5.74 (2,229)	0.02	NP<HC	3.85 (2,229)	0.055	
Superior Frontal	9.59 (2,229)	0.003	NP<HC	6.40 (2,229)	0.012	NP<HC
Caudal Middle Frontal	3.22 (2,229)	0.074		1.91 (2,229)	0.189	
Rostral Middle Frontal	4.49 (2,229)	0.033		2.79 (2,229)	0.097	
Par Opercularis	4.94 (2,229)	0.027		7.33 (2,229)	0.01	NP<HC
Pars Orbitalis	5.42 (2,229)	0.021		3.25 (2,229)	0.074	
Pars Triangularis	6.62 (2,229)	0.012	PP>NP§	7.46 (2,229)	0.01	NP<HC
Caudal Anterior Cingulate	0.53 (2,229)	0.619		1.03 (2,229)	0.385	
Rostral Anterior Cingulate	0.46 (2,229)	0.657		2.84 (2,229)	0.096	
Lateral Orbitofrontal	4.06 (2,229)	0.048		3.70 (2,229)	0.06	
Medial Orbitofrontal	2.94 (2,229)	0.089		2.13 (2,229)	0.158	
Frontal Pole	1.99 (2,229)	0.177		1.69 (2,229)	0.216	
Insula	3.34 (2,229)	0.074		2.5 (2,229)	0.124	
Superior Temporal	2.17 (2,229)	0.156		3.35 (2,229)	0.074	
Middle Temporal	6.28 (2,229)	0.012	NP<HC	5.55 (2,229)	0.02	NP<HC
Inferior Temporal	2.39 (2,229)	0.134		3.11 (2,229)	0.079	
Transverse Temporal	1.69 (2,229)	0.216		3.45 (2,229)	0.066	
Parahippocampal	6.37 (2,229)	0.012	PP<HC NP<HC	5.31 (2,229)	0.023	PP<HC
Entorhinal	4.95 (2,229)	0.027	PP<HC NP<HC	1.37 (2,229)	0.286	
Fusiform	7.12 (2,229)	0.01	NP<HC	4.73 (2,229)	0.03	NP<HC
Bank of Superior Temporal Sulcus	1.62 (2,229)	0.226		1.72 (2,92.97)	0.216	
Temporal pole	1.31 (2,229)	0.296		0.27 (2,229)	0.775	
Superior Parietal	5.47 (2,229)	0.021	NP<HC	4.77 (2,229)	0.028	NP<HC
Inferior Parietal	4.02 (2,229)	0.048	NP<HC	3.14 (2,85.97)	0.083	
Posterior Cingulate	0.13 (2,229)	0.88		3.33 (2,229)	0.074	
Isthmus Cingulate	1.88 (2,229)	0.19		3.27 (2,229)	0.074	
Supramarginal	2.21 (2,229)	0.153		2.37 (2,229)	0.14	
Precuneus	3.52 (2,229)	0.066		4.61 (2,229)	0.031	

F = F statistic of the group (PP, NP, HC) in the Analysis of Covariance (ANCOVA)/Welch's ANOVA test, *df* = degrees of freedom, PP = Positive-Pr dominant, NP = Negative-Predominant, HC = Healthy Control
*False Discovery Rate (FDR) corrected p-values, significant if ≤0.05
Post-hoc = Bonferroni test for inter-group differences
§ Trend level significance (p = 0.08) in Bonferroni test

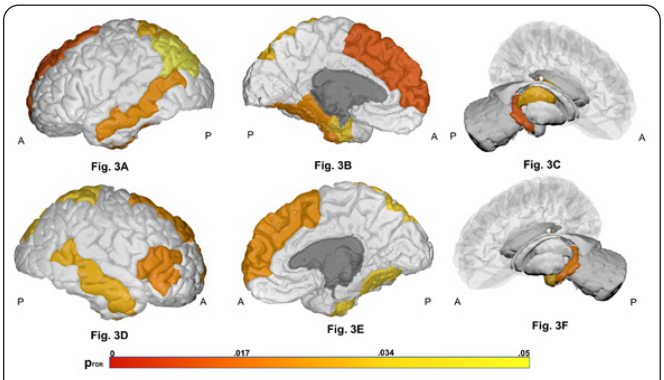

Figure 3: (From left to right) Lateral and medial views of the cortex and, the sub-cortex of the left (3A-C) and the right hemispheres (3D-F) of the brain. The yellow-orange areas are significantly smaller in Negative-Predominant Schizophrenia compared to healthy controls ($p_{FDR} \leq 0.05$), the white areas are either non-significant ($p_{FDR} > 0.05$) or not compared in the analysis.
A = Anterior, P = Posterior, FDR = False Discovery Rate

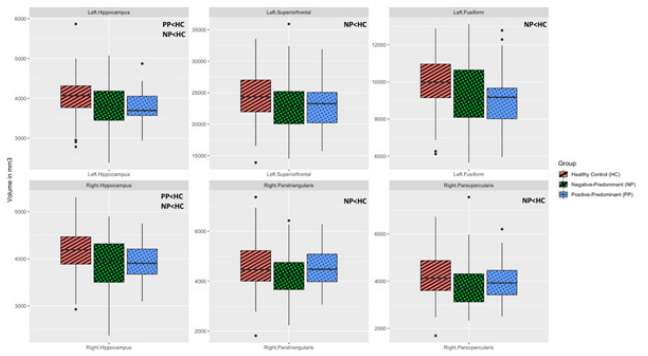

Figure 5: Box plots showing the distribution of volumes of brain regions in the 3 groups ($p_{FDR} \leq 0.01$). Also see supplemental figure 2 for other brain areas ($0.01 < p_{FDR} \leq 0.05$).

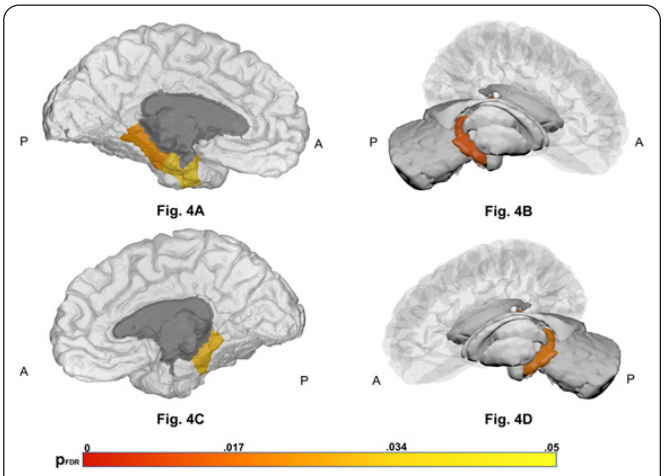

Figure 4: (From left to right) Medial views of the cortex and the sub-cortex of the left (4A-B) and the right hemispheres (4C-D) of the brain. The yellow-orange areas are significantly smaller in Positive-Predominant Schizophrenia compared to healthy controls ($p_{FDR} \leq 0.05$), the white areas are either non-significant ($p_{FDR} > 0.05$) or not compared in the analysis.
A = Anterior, P = Posterior, FDR = False Discovery Rate

Discussion

Through this study, with data freely gathered from open neuroimaging sources, we have demonstrated that symptomatically different subsets of patients of schizophrenia differ in brain structure compared to healthy controls. Schizophrenia patients having predominantly negative symptoms have widespread cortical decreases of volume involving regions in the frontal, temporal, and parietal lobes along with volumetric decreases of hippocampus, amygdala and the thalamus. Patients with predominantly positive symptoms have selective volume loss of bilateral medial temporal lobar structures compared to healthy controls.

Differences in brain structure amongst symptomatically different subsets of patients of schizophrenia have been explored before. A few relatively older studies proposed the temporolimbic system theory of paranoid schizophrenia [46-48] which attributes the positive symptoms of schizophrenia like the delusions and thought disorders to left-sided medial temporal lobe structures, especially the left hippocampal formation and parahippocampal gyrus. They also propose that a widespread and bilateral involvement of the frontal, temporal and parietal cortices is required for manifestation of negative symptoms accompanied by cognitive impairment. The volume of parahippocampal gyrus negatively correlated with the total positive symptom, delusional and conceptual disorganization scores, and were smaller in delusional patients than non-delusional patients of schizophrenia [49], further implicating its role in positive symptoms of schizophrenia. The hippocampus has been strongly linked to the pathogenesis of attenuated psychotic symptoms and transition to syndromal psychosis from clinical high risk in schizophrenia [50, 51]. Thus, our findings of medial temporal lobar involvement underlying positive symptoms of schizophrenia supports the findings from a broad time range of studies.

The medial temporal lobe has also been implicated in negative symptoms of schizophrenia [15, 52, 53] as is true with our findings. A few authors have suggested that atrophy of certain cortical structures in the frontal [54, 55] and temporal lobes [56] beyond a certain critical point is unconducive for the development of positive symptoms like delusions, which are minimal or absent in our sample of schizophrenia with predominant negative symptoms. Our findings of increased volume of Left parstriangularis in the PP compared to the NP albeit at trend level, statistically stands in support of this conceptualization. Benoit et al. provides a summary of structural studies comparing the deficit syndrome schizophrenia [57] comprising of patients with primary negative symptoms, with non-deficit schizophrenia. The results show that the differences between the deficit and the non-deficit types are mixed. A few studies implicate volume reductions in the frontal and temporal lobes to differentiate deficit from the non-deficit type [58, 59] but a few prove the contrary of greater structural abnormalities in non-deficit type [60, 61], some implicate only the temporal lobes [62, 63] and some the basal ganglia [64]. A few recent studies which have adopted novel methods of subtyping patients like maximum likelihood factor analysis have yielded similar results to ours [16, 18] with the paranoid group and disorganized subtypes demonstrating focal alterations whereas extensive cortical, limbic and subcortical thinning

characterizing the negative subtype. Differences between the findings of some previous studies and ours can be attributed to inherent differences in methods of categorizing the patients which range from clinical subtyping in the early days followed by unique rating scales like the schedule for deficit syndrome (SDS) [57] to advanced statistical methods in the recent studies. Other reasons could be varying sample sizes and variations in imaging analysis methods.

These results support that schizophrenia might not be a unitary homogenous entity either phenotypically or biologically and support the dimensional model of psychosis [65]. As mentioned before different symptom dimensions mean different prognoses [6-8] and different treatment responses [4, 5, 10]. Differential involvement of structures in the brain can also reflect different neurodevelopmental processes and neuroprogression underlying particular symptom subtypes [66]. Exploring this heterogeneity further in other biological variables can help identify unique symptom predominance in patients early in prodrome/early psychosis, [67-69] which in turn can aid in prognosticating, predicting the course and developing novel tailored therapies targeting the early phases. Though clinical subtyping of schizophrenia has been removed in DSM-5 due to limited diagnostic stability, poor reliability and validity [70, 71], symptom dimensions have supplanted clinical subtyping and is indicative of heterogeneity. Future studies can attempt classification of patients based on their dimensional scores and study neurobiological underpinnings of the classes derived based on dimensional scores.

Some of the major strengths of our study are that we have uniquely and effectively neutralized the variance introduced by multiple scanner hardware and image acquisition protocols of multiple projects, while simultaneously preserving the variance due to biological factors through ComBat, whose robustness over other traditional techniques has been established. This method has been used by very few multi-site structural studies so far. There has been a recent increase in the number of studies in psychiatry capitalizing on open source neuroimaging datasets [72, 73] with certain advantages like the findings being easily replicable, verifiable and more generalizable as they are derived from multiple populations. The possibility of unequal sample sizes statistically influencing the results has been addressed by application of appropriate statistical methods. Other studies which have examined neural substrates of symptom dimensions of schizophrenia have used ways of classifying patients according to the Schedule for Deficit Syndrome (SDS), factor analysis, cluster analysis or multivariate linear regression. These methods can still introduce heterogeneity within groups, for example in the deficit versus non-deficit syndrome classification, though the deficit group can include only patients with enduring negative symptoms, the non-deficit group can include everyone else who is not primarily negative including remitted patients and hence create inhomogeneity. Whereas, in our study we adopted a simple, yet reference based and unique way of classifying the patients into positive and negative predominant classes which can potentially resemble a clinician's classification regardless of clinical assessment battery used. This kind of classification is more specific to the symptom dimensions as there are no fully remitted patients in either group, the symptoms are unique and specific to each group and thus can potentially provide a more accurate result of association of symptom dimensions and neuroanatomical patterns. The high concordance observed between this classificatory method and an agnostic machine learning algorithm like the k-means clustering, adds to the validity of this classificatory method.

Another possible inference might be that there are no unique structural brain signatures of the symptom dimensions as there are no significant differences between the 2 groups. Results showed a larger volume of the Left parstriangularis in PP compared to the NP, albeit at trend level statistically. This can be due to the relatively smaller sample size of the PP resulting in inadequate power. The smaller sample size of PP may be attributable to the logistical difficulties in recruiting patients with more severe positive symptomatology into imaging studies and hence studies with a larger sample size can clarify the results. Advanced methods emerging from machine learning which potentially can pick up patterns in biological data more efficiently than traditional statistical techniques [24, 25] have emphasized the potential impact of phenotypic heterogeneity on imaging findings and need to be undertaken on a larger scale. Other potential covariates like duration of illness, age of onset of psychosis, co-morbid psychiatric and medical disorders and medication details were unavailable for all the subjects of all the projects in a uniform way and hence not included in the analysis. We did not include the other groups of patients (fully remitted; having both positive and negative symptoms) in the analysis as our aim was to study structural imaging findings specific to symptom dimensions.

Conclusion

This study demonstrates the structural brain differences associated with different symptom profiles of schizophrenia in an open neuroimaging database, using novel multi-site imaging data harmonization techniques. Further studies can be carried out in larger sample sizes, using more novel methods of symptom classification and imaging analysis, as well as using the regions implicated to measure possible disease progression or as markers of therapeutic response.

Conflicts of Interest

FAP is a consultant for and has equity in Imij Technologies and has several granted patents and applications in neuroimaging unrelated to this study. RB, JF and XF declare no conflicts of interest.

Acknowledgments

COBRE: Data was downloaded from the Collaborative Informatics and Neuroimaging Suite Data Exchange tool (COINS; http://coins.mrn.org/dx) and data collection was performed at the Mind Research Network and funded by a Center of Biomedical Research Excellence (COBRE) grant

5P20RR021938/P20GM103472 from the NIH to Dr. Vince Calhoun.

fBIRN: Data used for this study were downloaded from the Function BIRN Data Repository (http://fbirnbdr.birncommunity.org:8080/BDR/), supported by grants to the Function BIRN (U24-RR021992) Testbed funded by the National Center for Research Resources at the National Institutes of Health, U.S.A.

MCIC: Data used for this study were obtained from the Mind Clinical Imaging Consortium database through the Mind Research Network (www.mrn.org), a project supported by the Department of Energy, Award Number DE-FG02-08ER64581 which is a collaboration between investigators from the University of Iowa, University of Minnesota, University of New Mexico and Massachusetts General Hospital.

NUSDAST: Data used in this study were obtained from the NU Schizophrenia Data and Software Tool (NUSDAST) database (http://central.xnat.org/REST/projects/NUDataSharing), data collection and sharing for this project was funded by NIMH grant 1R01MH084803.The NUSDAST investigators' contribution is restricted to the design and implementation of NUSDAST and/or provision of data but did not participate in analysis or writing of this report.

This research did not receive any specific grant from funding agencies in the public, commercial, or not-for-profit sectors.

References

1. Wu EQ, Shi L, Birnbaum H, Hudson T, Kessler R. 2006. Annual prevalence of diagnosed schizophrenia in the USA: a claims data analysis approach. *Psychol Med* 36(11): 1535-1540. https://doi.org/10.1017/S0033291706008191
2. Charlson FJ, Ferrari AJ, Santomauro DF, Diminic S, Stockings F, et al. 2018. Global epidemiology and burden of schizophrenia: findings from the global burden of disease study 2016. *Schizophr. Bull* 44(6): 1195-1203. https://doi.org/10.1093/schbul/sby058
3. Andreasen NC, Carpenter WT.1993. Diagnosis and classification of schizophrenia. *Schizophr Bull* 19(2): 199-214. https://doi.org/10.1093/schbul/19.2.199
4. Garver DL, Holcomb JA, Christensen JD. 2000. Heterogeneity of response to antipsychotics from multiple disorders in the schizophrenia spectrum. *J Clin Psychiatry* 61(12): 964-972. https://doi.org/10.4088/jcp.v61n1213
5. Patel R, Jayatilleke N, Broadbent M, Chang CK, Foskett N, et al. 2015. Stewart, negative symptoms in schizophrenia: a study in a large clinical sample of patients using a novel automated method. *BMJ Open* 5(9): e007619. https://doi.org/10.1136/bmjopen-2015-007619
6. Fenton WS, McGlashan TH. 1991. Natural history of schizophrenia subtypes. II. Positive and negative symptoms and long-term course. *Arch Gen Psychiatry* 48(11): 978-986. https://doi.org/10.1001/archpsyc.1991.01810350018003
7. Goodman AB. 1989. Paranoid schizophrenia: prognosis under DSM-II and DSM-III-R. *Compr Psychiatry* 30(3): 259-266. https://doi.org/10.1016/0010-440x(89)90047-3
8. Kanahara N, Yoshida T, Oda Y, Yamanaka H, Moriyama T, et al. 2013. Onset pattern and long-term prognosis in schizophrenia: 10-year longitudinal follow-up study. *PloS One* 8(6) e67273. https://doi.org/10.1371/journal.pone.0067273
9. Villalta-Gil V, Vilaplana M, Ochoa S, Haro JM, Dolz M, et al. 2006. Neurocognitive performance and negative symptoms: are they equal in explaining disability in schizophrenia outpatients? *Schizophr Res* 87(1-3): 246-253. https://doi.org/10.1016/j.schres.2006.06.013
10. Fusar-Poli P, Papanastasiou E, Stahl D, Rocchetti M, Carpenter W, et al. 2015. Treatments of negative symptoms in schizophrenia: meta-analysis of 168 randomized placebo-controlled trials. *Schizophr Bull* 41(4): 892-899. https://doi.org/10.1093/schbul/sbu170
11. Brugger SP, Howes OD. 2017. Heterogeneity and homogeneity of regional brain structure in schizophrenia: a meta-analysis. *JAMA Psychiatry* 74(11): 1104-1111. https://doi.org/10.1001/jamapsychiatry.2017.2663
12. Zhang T, Koutsouleris N, Meisenzahl E, Davatzikos C. 2015. Heterogeneity of structural brain changes in subtypes of schizophrenia revealed using magnetic resonance imaging pattern analysis. *Schizophr Bull* 41(1): 74-84. https://doi.org/10.1093/schbul/sbu136
13. Dickinson D, Pratt DN, Giangrande EJ, Grunnagle M, Orel J, et al. 2018. Attacking heterogeneity in schizophrenia by deriving clinical subgroups from widely available symptom data. *Schizophr Bull* 44(1): 101-113. https://doi.org/10.1093/schbul/sbx039
14. Takahashi S. 2017. Heterogeneity of schizophrenia: genetic and symptomatic factors. *Am J Med Genet Part B Neuropsychiatr* Genet 162(7): 648-652. https://doi.org/10.1002/ajmg.b.32161
15. Benoit A, Bodnar M, Malla AK, Joober R, Lepage M. 2012. The structural neural substrates of persistent negative symptoms in first-episode of non-affective psychosis: a voxel-based morphometry study. *Front Psychiatry* 3: 42. https://doi.org/10.3389/fpsyt.2012.00042
16. Koutsouleris N, Gaser C, Jäger M, Bottlender R, Frodl T, et al. 2009. Structural correlates of psychopathological symptom dimensions in schizophrenia: a voxel-based morphometric study, *NeuroImage* 39(4): 1600-1612. https://doi.org/10.1016/j.neuroimage.2007.10.029
17. Nenadic I, Sauer H, Gaser C. 2010. Distinct pattern of brain structural deficits in subsyndromes of schizophrenia delineated by psychopathology. *NeuroImage* 49(20): 1153-1160. https://doi.org/10.1016/j.neuroimage.2009.10.014
18. Nenadic I, Yotter RA, Sauer H, Gaser C. 2015. Patterns of cortical thinning in different subgroups of schizophrenia. *Br J Psychiatry* 206(6): 479-483. https://doi.org/10.1192/bjp.bp.114.148510
19. Voineskos AN, Foussias G, Lerch J, Felsky D, Remington G, et al. 2013. Neuroimaging evidence for the deficit subtype of schizophrenia. *JAMA Psychiatry* 70(5): 472–480. https://doi.org/10.1001/jamapsychiatry.2013.786
20. Weinberg D, Lenroot R, Jacomb I, Allen K, Bruggemann J, et al. 2016. Cognitive subtypes of schizophrenia characterized by differential brain volumetric reductions and cognitive decline. *JAMA Psychiatry* 73(12): 1251-1259. https://doi.org/10.1001/jamapsychiatry.2016.2925
21. Wheeler AL, Wessa M, Szeszko PR, Foussias G, Chakravarty MM,et al. 2015. Further neuroimaging evidence for the deficit subtype of schizophrenia: a cortical connectomics analysis. *JAMA Psychiatry* 72(5) 446-455. https://doi.org/10.1001/jamapsychiatry.2014.3020
22. Walton E, Hibar DP, van Erp TGM, Potkin SG, Roiz-Santiañez R, et al. 2017. Positive symptoms associate with cortical thinning in the superior temporal gyrus via the ENIGMA Schizophrenia consortium. *Acta Psychiatr Scand* 135(5): 439-447. https://doi.org/10.1111/acps.12718
23. Walton E, Hibar DP, van Erp TGM, Potkin SG, Roiz-Santiañez R, et al. 2018. Prefrontal cortical thinning links to negative symptoms in schizophrenia via the ENIGMA consortium, *Psychol Med* 48(1): 82-94. https://doi.org/10.1017/S0033291717001283
24. Dwyer DB, Cabral C, Kambeitz-Ilankovic L, Sanfelici R, Kambeitz J, et al. 2018. Brain subtyping enhances the neuroanatomical discrimination of schizophrenia. *Schizophr Bull* 44(5): 1060-1069. https://doi.org/10.1093/schbul/sby008
25. Rozycki M, Satterthwaite TD, Koutsouleris N, Erus G, Doshi J, et al. 2018. Multisite machine learning analysis provides a robust structur-

al imaging signature of schizophrenia detectable across diverse patient populations and within individuals. *Schizophr Bull* 44(5): 1035-1044. https://doi.org/10.1093/schbul/sbx137

26. Hanlon FM, Houck JM, Pyeatt CJ, Lundy SL, Euler MJ, et al. 2011. Bilateral hippocampal dysfunction in schizophrenia. *NeuroImage* 58(4): 1158-1168. https://doi.org/10.1016/j.neuroimage.2011.06.091
27. Gollub RL, Shoemaker JM, King MD, White T, Ehrlich S, et al. 2013. The MCIC collection: a shared repository of multi-modal, multi-site brain image data from a clinical investigation of schizophrenia. *Neuroinformatics.* 11(3): 367-388. https://doi.org/10.1007/s12021-013-9184-3
28. Keator DB, van Erp TGM, Turner JA, Glover GH, Mueller BA, et al. 2016. The function biomedical informatics research network data repository. *NeuroImage* 124(Pt B): 1074-1079. https://doi.org/10.1016/j.neuroimage.2015.09.003
29. Wang J, Zhou L, Cui C, Liu Z, Lu J. 2017. Gray matter morphological anomalies in the cerebellar vermis in first-episode schizophrenia patients with cognitive deficits. *BMC Psychiatry* 17(1): 374. https://doi.org/10.1186/s12888-017-1543-4
30. Andreasen NC. 1984. Scale for the assessment of negative symptoms/ scale for the assessment of positive symptoms [Manual]
31. Kay SR, Fiszbein A, Opler LA. 1987. The positive and negative syndrome scale (PANSS) for schizophrenia. *Schizophr Bull* 13(12): 261-276. https://doi.org/10.1093/schbul/13.2.261
32. van Erp TGM, Preda A, Nguyen D, Faziola L, Turner J, et al. 2014. Converting positive and negative symptom scores between PANSS and SAPS/SANS, *Schizophr Res* 152(1): 289-294. https://doi.org/10.1016/j.schres.2013.11.013
33. Andreasen NC, Carpenter WT, Kane JM, Lasser RA, Marder SR, et al. 2005. Remission in schizophrenia: proposed criteria and rationale for consensus. *Am J Psychiatry* 162: 441-449. https://doi.org/10.1176/appi.ajp.162.3.441
34. Ségonne F, Dale AM, Busa E, Glessner M, Salat D, et al. 2004. A hybrid approach to the skull stripping problem in MRI. *NeuroImage* 22(3): 1060-1075. https://doi.org/10.1016/j.neuroimage.2004.03.032
35. Ségonne F, Grimson E, Fischl B. 2005. A genetic algorithm for the topology correction of cortical surfaces *Inf Process Med Imaging* 19: 393-405. https://doi.org/10.1007/11505730_33
36. Ségonne F, Pacheco J, Fischl B. 2007. Geometrically accurate topology-correction of cortical surfaces using nonseparating loops. *IEEE Trans Med Imaging* 26(4): 518-529. https://doi.org/10.1109/TMI.2006.887364
37. Lancaster JL, Woldorff MG, Parsons LM, Liotti M, Freitas CS, et al. 2000. Automated Talairach atlas labels for functional brain mapping. *Hum Brain Mapp* 10(3): 120-131. https://doi.org/10.1002/1097-0193(200007)10:3<120::aid-hbm30>3.0.co;2-8
38. Fischl B, Sereno MI, Dale AM. 1999. Cortical surface-based analysis: II: Inflation, flattening, and a surface-based coordinate system. *NeuroImage* 9(2): 195-207. https://doi.org/10.1006/nimg.1998.0396
39. Desikan RS, Ségonne F, Fischl B, Quinn BT, Dickerson BC, et al. 2006. An automated labeling system for subdividing the human cerebral cortex on MRI scans into gyral based regions of interest. *NeuroImage* 31(3): 968-980. https://doi.org/10.1016/j.neuroimage.2006.01.021
40. Klein A, Tourville J. 2012. 101 Labeled brain images and a consistent human cortical labeling protocol. *Front Neurosci* 6: 171. https://doi.org/10.3389/fnins.2012.00171
41. Fischl B, Salat DH, Busa E, Albert M, Dieterich M, et al. 2002. Whole brain segmentation: automated labeling of neuroanatomical structures in the human brain. *Neuron* 33(3): 341-355. https://doi.org/10.1016/s0896-6273(02)00569-x
42. Johnson WE, Li C, Rabinovic A. 2007. Adjusting batch effects in microarray expression data using empirical Bayes methods. *Biostatistics* 8(1): 118-127. https://doi.org/10.1093/biostatistics/kxj037
43. Fortin JP, Parker D, Tunç B, Watanabe T, Elliott MA, et al. 2017. Harmonization of multi-site diffusion tensor imaging data. *NeuroImage* 161: 149-170. https://doi.org/10.1016/j.neuroimage.2017.08.047
44. Fortin JP, Cullen N, Sheline YI, Taylor WD, Aselcioglu I, et al. 2018. Harmonization of cortical thickness measurements across scanners and sites. *NeuroImage* 167: 104-120. https://doi.org/10.1016/j.neuroimage.2017.11.024
45. Andy Field, Jeremy Miles, Zoe Field, 2012. Discovering statistics using R. SAGE publications, Los Angeles, London, New Delhi, Singapore, Washington DC, USA.
46. Bogerts B. 1997. The temporolimbic system theory of positive schizophrenic symptoms, *Schizophr Bull* 23(3): 423-435. https://doi.org/10.1093/schbul/23.3.423
47. Casanova F. 1997. The temporolimbic system theory of paranoid schizophrenia. *Schizophr. Bull* 23(3): 513-515. https://doi.org/10.1093/schbul/23.3.513
48. Olney JW, Farber NB. 1997. Discussion of Bogerts' temporolimbic system theory of paranoid schizophrenia. *Schizophr Bull* 23(3): 533-536. https://doi.org/10.1093/schbul/23.3.533
49. Prasad KMR, Rohm BR, Keshavan MS. 2004. Parahippocampal gyrus in first episode psychotic disorders: a structural magnetic resonance imaging study. *Prog Neuropsychopharmacol Biol Psychiatry* 28(4): 651-658. https://doi.org/10.1016/j.pnpbp.2004.01.017
50. Lieberman JA, Girgis RR, Brucato G, Moore H, Provenzano F, et al. 2018. Hippocampal dysfunction in the pathophysiology of schizophrenia: a selective review and hypothesis for early detection and intervention. *Mol Psychiatry* 23(8): 1764-1772. https://doi.org/10.1038/mp.2017.249
51. Provenzano FA, Guo J, Wall MM, Feng X, Sigmon HC, et al. 2020. Hippocampal pathology in clinical high-risk patients and the onset of schizophrenia. *Biol Psychiatry* 87(3): 234-242. https://doi.org/10.1016/j.biopsych.2019.09.022
52. Anderson JE, Wible CG, McCarley RW, Jakab M, Kasai K, et al. 2002. An MRI study of temporal lobe abnormalities and negative symptoms in chronic schizophrenia. *Schizophr Res* 58(2-3): 123-134. https://doi.org/10.1016/s0920-9964(01)00372-3
53. Sigmundsson T, Suckling J, Maier M, Williams S, Bullmore E, et al. 2001. Structural abnormalities in frontal, temporal, and limbic regions and interconnecting white matter tracts in schizophrenic patients with prominent negative symptoms. *Am J Psychi*atry 158(2): 234-243. https://doi.org/10.1176/appi.ajp.158.2.234
54. Nasrallah HA, Rizzo M, Damasio H, McCalley-Whitters M, Kuperman S, et al. 1982. Neurological differences between paranoid and nonparanoid schizophrenia: part II. computerized tomographic findings, *J Clin Psychiatry* 43(8): 307-309.
55. Whitford TJ, Farrow TFD, Williams LM, Gomes L, Brennan J, et al. 2009. Delusions and dorso-medial frontal cortex volume in first-episode schizophrenia: a voxel-based morphometry study, *Psychiatry Res Neuroimaging* 172(3): 175-179. https://doi.org/10.1016/j.pscychresns.2008.07.011
56. Menon RR, Barta PE, Aylward EH, Richards SS, Vaughn DD, et al. 1995. Posterior superior temporal gyrus in schizophrenia: grey matter changes and clinical correlates. *Schizophr Res* 16(2): 127-135. https://doi.org/10.1016/0920-9964(94)00067-i
57. Kirkpatrick B, Buchanan RW, McKenney PD, Alphs LD, Carpenter WT. 1989. The schedule for the deficit syndrome: an instrument for research in schizophrenia. *Psychiatry Res* 30(2): 119-123. https://doi.org/10.1016/0165-1781(89)90153-4
58. Cascella NG, Fieldstone SC, Rao VA, Pearlson GD, Sawa A, et al. 2010. Gray-matter abnormalities in deficit schizophrenia, *Schizophr Res* 120(1-3): 63-70. https://doi.org/10.1016/j.schres.2010.03.039
59. Fischer BA, Keller WR, Arango C, Pearlson GD, McMahon RP, et al. 2012. Cortical structural abnormalities in deficit versus nondeficit

schizophrenia. *Schizophr Res* 136(1-3): 51-54. https://doi.org/10.1016/j.schres.2012.01.030

60. Quarantelli M, Larobina M, Volpe U, Amati G, Tedeschi E, et al. 2002. Stereotaxy-based regional brain volumetry applied to segmented MRI: validation and results in deficit and nondeficit schizophrenia, *Neuroimage* 17 (1): 373-384. https://doi.org/10.1006/nimg.2002.1157
61. Volpe U, Mucci A, Quarantelli M, Galderisi S, Maj M. 2012. Dorsolateral prefrontal cortex volume in patients with deficit or nondeficit schizophrenia. *Prog Neuropsychopharmacol Biol Psychiatry* 37(2): 264-269. https://doi.org/10.1016/j.pnpbp.2012.02.003
62. Galderisi S, Quarantelli M, Volpe U, Mucci A, Cassano GB, et al. 2008. Patterns of structural MRI abnormalities in deficit and nondeficit schizophrenia. *Schizophr Bull* 34(2): 393-401. https://doi.org/10.1093/schbul/sbm097
63. Turetsky B, Cowell PE, Gur RC, Grossman RI, Shtasel DL, et al. 1995. Frontal and temporal lobe brain volumes in schizophrenia: relationship to symptoms and clinical subtype. *Arch Gen Psychiatry* 52(12): 1061-1070. https://doi.org/10.1001/archpsyc.1995.03950240079013
64. Buchanan RW, Breier A, Kirkpatrick B, Elkashef A, Munson RC, et al. 1993. Structural abnormalities in deficit and nondeficit schizophrenia. *Am J Psychiatry* 150(1): 59-65. https://doi.org/10.1176/ajp.150.1.59
65. Tandon R, Nasrallah HA, Keshavan MS. 2009. Schizophrenia, "just the facts" 4. clinical features and conceptualization *Schizophr Res* 110(1-3): 1-23. https://doi.org/10.1016/j.schres.2009.03.005
66. Pantelis C, Yücel M, Wood SJ, Velakoulis D, Sun D, et al. 2005. Structural brain imaging evidence for multiple pathological processes at different stages of brain development in schizophrenia. *Schizophr Bull* 31(3): 672-696. https://doi.org/10.1093/schbul/sbi034
67. Lyne J, Renwick L, Madigan K, O'Donoghue B, Bonar M, et al. 2014. Do psychosis prodrome onset negative symptoms predict first presentation negative symptoms?, Eur Psychiatry 29(3): 153-159. https://doi.org/10.1016/j.eurpsy.2013.02.003
68. Moukas G, Stathopoulou A, Gourzis P, Beratis IN, Beratis S. 2010. Relationship of "prodromal" symptoms with severity and type of psychopathology in the active phase of schizophrenia. *Compr Psychiatry* 51(1): 1-7. https://doi.org/10.1016/j.comppsych.2009.02.001
69. Piskulic D, Addington J, Cadenhead KS, Cannon TD, Cornblatt BA, et al. 2012. Negative symptoms in individuals at clinical high risk of psychosis. *Psychiatry Res* 196(2-3): 220-224. https://doi.org/10.1016/j.psychres.2012.02.018
70. Mattila T, Koeter M, Wohlfarth T, Storosum J, van den Brink W, et al. 2015. Impact of DSM-5 changes on the diagnosis and acute treatment of schizophrenia. *Schizophr Bull* 41(3): 637-643. https://doi.org/10.1093/schbul/sbu172
71. Tandon R.2014. Schizophrenia and other psychotic disorders in diagnostic and statistical manual of mental disorders (DSM)-5: Clinical implications of revisions from DSM-IV. *Indian J Psychol Med* 36(3): 223. https://doi.org/10.4103/0253-7176.135365
72. Oh J, Oh BL, Lee KU, Chae JH, Yun K. 2020. Identifying schizophrenia using structural MRI with a deep learning algorithm. *Front Psychiatry* 11: 16. https://doi.org/10.3389/fpsyt.2020.00016
73. Basavaraju R, Feng X, France J, Huey ED, Provenzano FA, et al. 2020. Depression is associated with preserved cortical thickness relative to apathy in frontotemporal dementia. *J Geriatr Psychiatry Neurol* October 08, 20. https://doi.org/10.1177/0891988720964258